Vol. 89: 1–14, 2022
https://doi.org/10.3354/cr01701

CLIMATE RESEARCH
Clim Res

Published online October 13

Role of changing land use and land cover (LULC) on the 2018 megafloods over Kerala, India

Ankur Dixit[1,*], Sandeep Sahany[1,2], Balaji Rajagopalan[3,4], Sweta Choubey[1]

[1]Centre for Atmospheric Sciences, Indian Institute of Technology Delhi 110016, India
[2]Centre for Climate Research, 537054 Singapore
[3]Department of Civil, Environmental, and Architectural Engineering, University of Colorado, Boulder, CO 80309, USA
[4]Cooperative Institute for Research in Environmental Sciences (CIRES), University of Colorado, Boulder, CO 80309, USA

ABSTRACT: The state of Kerala, India, experienced massive flooding in August 2018. Unprecedented extreme rainfall left the region with huge losses of infrastructure. Several studies reported the role of improper dam operations and climate change in this region. However, changing land use/land cover (LULC) is an important driver of flood modulation; we therefore studied regional LULC changes (over 4 decades) and their impacts on flooding during this event using the Weather Research Forecasting (WRF)-Hydro model. We downscaled the NCEP final operational global analysis data using WRF to provide meteorological inputs for the gridded WRF-Hydro model. WRF downscaled forcing, along with observed discharge, were used to calibrate WRF-Hydro, which was run with the meteorological forcing of the August 2018 floods using LULC corresponding to 1985, 1995, 2005, and 2018. Analysis of LULC change indicated a significant loss of evergreen forest and reductions in shrubland during 1995–2005 and considerable loss of mixed forest during 2005–2018. The most extensive changes in flooding attributes (discharge, inundation area, and flood surface height) were found for LULC changes from 1995 to 2005. Specifically, comparing 2005 to 1995, we found that high flows (estimated by Q_{10}) increased by >10 % at many stations (up to ~50 % for several locations). The increase in surface water head was ~40 % over some parts with increased inundation. During 2005–2018, afforestation measures reduced the steep decline in LC observed during 1995–2005. Thus, the contribution of LULC changes to the August 2018 flooding is mainly due to the deforestation-related changes during 1995–2005. This substantial role of LC in enhancing flood hazards highlights the need to better manage LC in watersheds.

KEY WORDS: Kerala Flood 2018 · Weather Research Forecasting · WRF · WRF-Hydro · Flood modeling · Land use/land cover change · LULC change · Deforestation

1. INTRODUCTION

In recent years, record-breaking rainfall events have occurred worldwide that have severely affected the environment and human society (Lehmann et al. 2015). Such events often lead to floods, causing massive destruction of infrastructure with detrimental impacts on the economy, ecology, and environment. Global warming plays a significant part in the magnitude and frequency of such unprecedented extreme events (Diffenbaugh et al. 2017). The Fifth Assessment Report (AR5) of the IPCC confirmed the influence of humans on the climate system and changes in frequency and intensity of extreme weather and climate events since 1950 (Alexander et al. 2006, Allan & Soden 2008, Stott et al. 2016). A warmer atmosphere leads to increased water vapor, resulting in a greater probability of extreme precipitation and subsequent floods (IPCC 2007). India is no exception to this worldwide trend

*Corresponding author: ankur.dixit@cas.iitd.ac.in

Publisher: Inter-Research · www.int-res.com

and has witnessed a significant rise in extreme events. Goswami et al. (2006) observed a significant increasing trend in extreme events and a decreasing trend in the frequency of moderate events frequency over central India, although they did not find a significant trend in mean annual rainfall. During 1950–2015, there was a threefold increase in extreme rain events over central India due to the increasing variability and strength of the low-level monsoon westerlies (Roxy et al. 2017). Because of these extreme events, flooding continues to be one of the most catastrophic natural hazards globally (Bubeck et al. 2017)

Rapid changes in land use/land cover (LULC) have led to widespread degradation and loss of tropical ecosystems, affecting agriculture and ecological processes (Millennium Ecosystem Assessment 2005, FAO 2011). The dynamics of LULC play a critical role in the hydrological balance, including surface runoff, subsurface runoff, groundwater recharge, and other terrestrial fluxes (Novotny & Olem 1994, Bhaduri et al. 2000, Weng 2001, Frumkin 2002, Li & Wang 2009, Zhu & Li 2014) and potentially contribute to flooding signatures. The transition of natural land cover such as forests and shrubs into croplands or urban areas affects land permeability and alters the hydrological regime. Therefore, changes in LULC might explain some of the problems in river basins (Mayaja & Srinivasa 2016). LULC changes also induce variations in rooting depth, albedo, surface roughness, and various other hydrological parameters (Chahine 1992, Mahmood et al. 2010, Frans et al. 2013) that may contribute to flooding events.

Several studies have highlighted that changes in LULC alter the physical properties of land surfaces and vegetation and affect streamflow, sediment yield, evapotranspiration, and other fluxes (Petchprayoon et al. 2010, Zhu & Li 2014, Wu et al. 2015, Welde & Gebremariam 2017). Although both changing climate and land use are responsible for increased runoff, land-use change is a more decisive factor, especially in the tropics (Piao et al. 2007). Urban sprawl was a vital factor behind the increased runoff over the upper San Pedro watershed, USA, from 1973 to 1997 (Nie et al. 2011). LULC changes in the Oshiwara River Basin in Mumbai, India, over the last 4 decades led to increased peak and total runoff volume (Zope et al. 2016). That study estimated an increment of up to 64% in the areal extent of the flood hazard zone from 1966 to 2009. In Kerala, the Pampa River Basin exhibited adverse effects on its ecology and aggravated flood and drought risks due to significant LULC changes and human intervention from 2001 to 2010 (Mayaja & Srinivasa 2016). A study of LULC change over 4 river basins in East India found increased runoff and baseflow with decreased evapotranspiration because of reduced vegetation cover from 1985 to 2005 (Das et al. 2018). These are representative studies that have found strong connections between LULC changes and hydrology of the river basins in India; other studies also add to this body of evidence.

Alterations to hydrological regimes in river basins contribute to various microclimate changes and affect their overall ecology. Therefore, changes in LULC and climate variability makes for a potent combination in producing more severe floods than the meteorology would warrant. Boyaj et al. (2020) reported that heavy rainfall events have increased by 20–25% due to LULC change over southern India (states of Kerala, Telangana, and Tamilnadu). They reported that LULC change is causing higher convective available potential energy because of increasing surface temperature and sensible heat fluxes.

In southern India, the state of Kerala experienced an extremely heavy rainfall event during August 2018, during which 1.5 million people were displaced (BBC News 2018: https://www.bbc.com/news/world-asia-india-45267014), and around 339 deaths were reported (Government of Kerala 2018) with an economic loss of about Indian Rupee ₹ 310–400 billion (Jayakumar 2018, Rajiv Gandhi Institute of Development Studies 2018, UNDP 2018, Hunt & Menon 2020). Another source reported 498 causalities due to flooding and subsequent landslides (JRDNA Team 2018). Mishra et al. (preprint doi:10.5194/hess-2018-480) reported that 1, 2, and 3 d rainfall accumulations (during this event) had 75, 200, and 100 yr return periods, respectively. They also reported that in the upstream region of 3 major reservoirs (Idukki, Kakki, and Periyar), the rainfall accumulation during 1–15 August 2018 had a return period of 500 yr. Interestingly, Kerala experienced a significant decline in monsoon season precipitation during 1951–2017, much like most of India, even with a rise in temperature during the period (Mishra & Shah 2018). The total runoff during the monsoon season for this period was also reported as having declined (Mishra & Shah 2018).

A report by the Western Ghats Ecology Expert Panel (WGEEP) indicated various human intervention activities in the eco-sensitive zones of Kerala and identified them as being vulnerable to the ecological development of the region (Gadgil et al. 2011). The report also suggested that the change in land use patterns in the Western Ghats has led to flow fluctuations, lower water tables, and water quality degradation. River course alteration due to the construction of dams has caused massive encroachment in forests and catchments (Gadgil et al. 2011). Studies on LULC changes in various parts of Kerala have also shown reductions in vegetated areas caused by increasing urbanization trends (Shaji et al. 2017, Prasad & Ramesh 2019). Various socio-economic changes have led to the fast rate of infrastructure development and real estate construction in Kerala. The introduction of the Land Reforms Act 1971 (Raj & Azeez 2010) further escalated this rate at the end of the 20th century.

Motivated by the literature discussed above and the major flooding event of 2018 in Kerala, in this study, we sought to answer the question: What is the role of LULC changes on the hydrological response of the August 2018 flood event? Answering this question can help to develop land-use strategies as part of flood mitigation efforts.

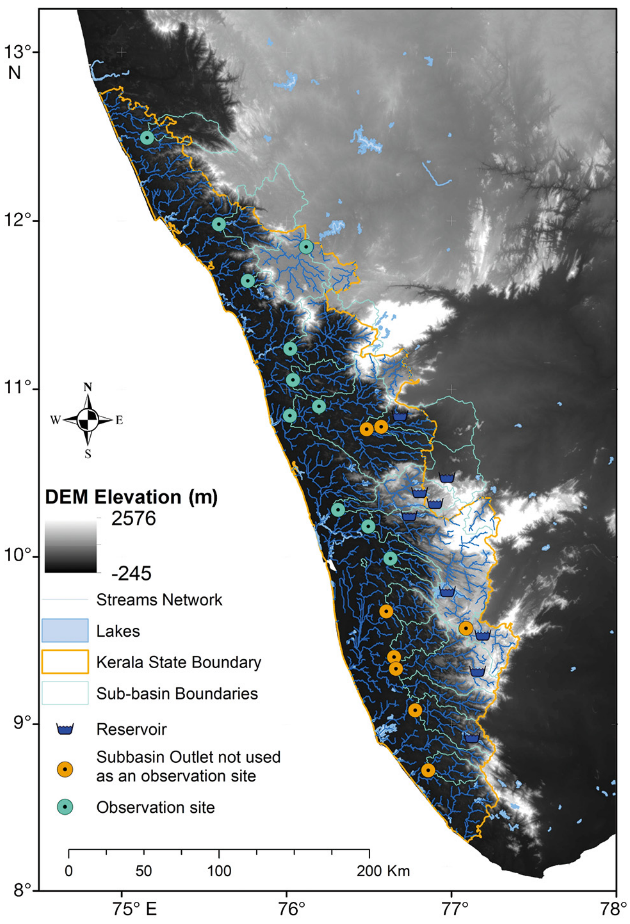

Fig. 1. Kerala, India, showing the topography, stream network, lakes, sub-basin boundaries, reservoirs, and state boundary. The state boundary is shown to emphasize that only stations lying within Kerala were used for analysis. DEM: digital elevation model

2. STUDY AREA

Kerala is located on the southwestern tip of India from latitudes 8° 15′ to 12° 50′ N and longitudes 74° 50′ to 77° 30′ E (Fig. 1). It is bounded by the Western Ghats chain (which occupies around 48 % of the total area of Kerala) in the east and the Arabian Sea in the west. The state comprises 3 physiographic regions that include highlands in the east (Western Ghats), midland plains in central Kerala, and the coastal belt in the west. The Western Ghats comprise one of India's major biodiversity hotspots, and therefore include ecologically sensitive zones. The WGEEP report demarcated the entire Western Ghats as an ecologically sensitive area (ESA) assigned under 3 ESA classification levels (Gadgil et al. 2011). The report also recommended that no new reservoirs of large capacity be constructed.

Kerala has a tropical monsoon climate with 4 seasons (summer, southwest monsoon, northeast monsoon, and winter) and receives around 3000 mm of rainfall annually due to its location on the western slopes of Western Ghats. From 1871 to 2012, the average annual rainfall over Kerala was 2827 mm, with a minimum of 1892 mm and a maximum of 4066 mm (Thomas & Prasannakumar 2016). Rainfall seasons, i.e. the southwest monsoon (June–September) and the northeast monsoon (October–December) contribute around 68 and 17.3 %, respectively, to the annual rainfall (Thomas & Prasannakumar 2016). Kerala has more than 40 reservoirs (India Water Resources Information System [WRIS]: https://indiawris.gov.in/wris/) and 44 rivers, of which 41 flow westward and 3 flow eastward.

3. MODEL, DATA, AND METHODS

We performed this study in 2 steps: LULC change assessment, followed by numerical simulations. We used Weather Research Forecasting (WRF) version 3.9.1.1 to simulate meteorological forcing that further fed WRF-Hydro version 5.0.3 in offline-coupled mode to simulate terrestrial hydrological processes.

3.1. Model configuration

3.1.1. WRF

WRF is a state-of-the-art model used for dynamical downscaling, numerical weather prediction, and atmospheric simulation (Wang et al. 2008). It is also suitable for other applications such as regional climate simulations, air quality modeling, atmosphere–ocean coupling, data assimilation development studies, parameterized physics research, and idealized simulations. WRF features non-hydrostatic dynamics with multi-nest capability, and provides physical parameterization schemes of varied sophistication for representing physical processes including surface and planetary boundary layer turbulence, atmospheric radiative transfer, and cloud formation.

We designed a 2-level, 1-way nested domain in this study (Fig. 2). The outer domain has a horizontal grid spacing of 25 km, with 172 grid points in the north–south direction and 233 grid points in the east–west direction. The inner domain has a horizontal grid spacing of 5 km, with 126 grid points in the north–south direction and 86 grid points in the east–west direction. We set 40 vertical levels for both domains with model top at 50 hPa. The initial condition and lateral boundary conditions are derived from the NCEP final operational global analysis (FNL) 6-hourly, 1-degree data (NCEP/NOAA/UD-DoC 2000) from 0000 UTC on 11 May 2016 to 0000 UTC on 12 September 2018 for the outer domain. Table 1 lists all of the physical parameterizations used in the WRF simulations. We used the WRF Single-Moment (WSM) 6-class graupel microphysics scheme, which is suitable for high-resolution simulations (Kumar et al. 2008) and best suited to simulate heavy precipitation events (Deb et al. 2008, Chevuturi & Dimri 2016). Several studies over India suggested that the Kain-Fritsch convection scheme performed better in simulating heavy precipitation events than other schemes (Deb et al. 2008, Chevuturi & Dimri 2016). The longwave and shortwave radiation schemes used were RRTM (Mlawer et al. 1997) and Dudhia (Dudhia 1989), respectively. The Noah-MP land surface model was used to maintain consistency to represent land surface processes across the experiment, using WRF-Hydro. The sea surface temperature update was incorporated at a 6 h interval and utilized adaptive time-stepping to avoid the run-time Courant-Friedrichs-Lewy (CFL) condition failure.

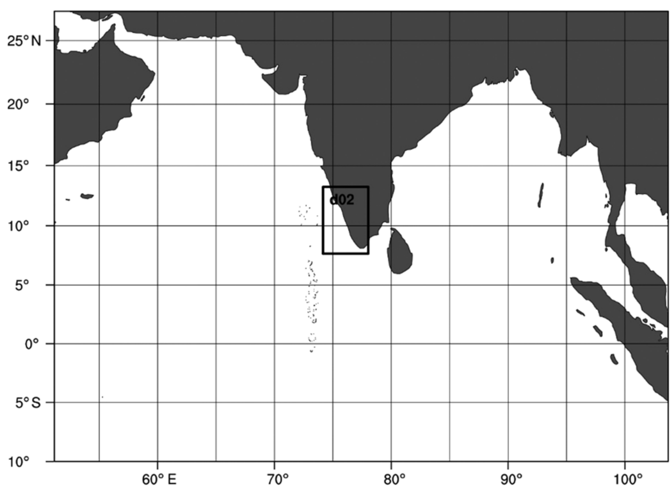

Fig. 2. Two-level nested Weather Research Forecasting (WRF) domain used in this study. The outer domain (d01, borders of the figure) has a horizontal grid spacing of 25 km with 172 grid points in the north–south direction and 233 grid points in the east–west direction. The inner domain (d02) has a horizontal grid spacing of 5 km, with 126 grid points in the north–south direction and 86 grid points in the east–west direction

3.1.2. WRF-Hydro

WRF-Hydro enables the simulation of terrestrial hydrological processes in online or offline coupling mode with atmospheric models. WRF-Hydro acts as a middle layer between weather/climate models and terrestrial hydrological models along with land data assimilation systems (Gochis et al. 2018). In this model, switch-activated modules are adapted and integrated to represent land surface physics and hydrological processes such as vertical land surface parameterization, surface overland flow, saturated subsurface flow, channel routing, reservoir routing, and conceptual base flow processes.

Table 1. Summary of Weather Research Forecasting (WRF) options used in the study. ARW: Advanced Research WRF; WSM: WRF single moment microphysics scheme; RRTM: Rapid Radiative Transfer Model; YSU: Yonsei University; Noah MP: Noah Multi-parameterization; FNL: NCEP Final Operational Global Analysis data; SST: sea surface temperature

Model attributes	Options used
Solver	ARW
Number of domains (grid spacing)	2: outer domain (25 km), inner domain (5 km); 1-way nesting
Microphysics scheme	WSM6 (Hong & Lim 2006)
Convection scheme	Kain-Fritsch (Kain 2004)
Longwave radiation scheme	RRTM (Mlawer et al. 1997)
Shortwave radiation scheme	Dudhia (Dudhia 1989)
Planetary boundary layer	YSU (Hong et al. 2006)
Land surface	Noah MP (Niu et al. 2011)
Surface layer option	Monin-Obukhov Similarity scheme (Cheng et al. 2005)
SST (update frequency)	FNL Analysis (6-hourly)
Adaptive time step	True
Number of land categories	24

We used 20 as an aggregation factor that brought down the routing grid size to 250 m. To simulate land surface processes, we chose the Noah-MP land surface model with 4 soil layers. We activated the switch to overland flow routing and opted for the steepest descent (D8) algorithm to regulate the flow. We employed a diffusive wave gridded routing algorithm to simulate channel routing and flows, which is a 1-dimensional diffusive wave formulated with a variable time-stepping and simplification of St. Venant equations for shallow-water waves. This routing algorithm is a first-order Newton-Raphson equation used to integrate diffusive wave flow equations that might raise some instabilities in areas with low gradient channel reaches. The study region has a channel reach gradient lying along the Western Ghats, so we employed this algorithm because of its capability to parameterize the reservoirs. In other algorithms, reservoir parameterization is yet to be supported. The model baseflow processes used an exponent bucket method.

3.2. LULC change assessment

We adhered to the United States Geological Survey (USGS) classification scheme to assess changes in LULC. We obtained LULC data from Bhuvan (Biswadip 2014; https://bhuvan.nrsc.gov.in), the Indian Space Research Organisation (ISRO), and decadal LULC across India (Roy et al. 2016). We selected the dominant classes over Kerala to assess the LULC change. The classes that we chose are Urban and Built-up Land (UBL), Dryland Cropland and Pasture (DCP), Irrigated Cropland and Pasture (ICP), Mixed Dryland/Irrigated Cropland and Pasture (MICP), Cropland/Grassland Mosaic (CGM), Cropland/Woodland Mosaic (CWM), Grassland (GL), Shrubland (SL), Evergreen Forest (EF), Mixed Forest (MF), and Barren or Sparsely Vegetated (BSV). In the USGS classification system, some classes might be inter-transitional over an extended period, such as decadal, leading to uncertainty. To avoid these uncertainties, we merged DCP, ICP, MICP, CGM, and CWM as Cropland and Pasture (CLP) to assess the notable changes in LULC that can have a significant impact on the hydrological regime in Kerala.

3.3. Numerical simulation

Following the LULC change assessment, we simulated high-resolution meteorological forcings using WRF with LULC for 1985, 1995, 2005, and 2018. These LULC datasets are ingested in the pre-processing under geogrid processing. The objective of ingesting LULC in WRF is to represent impacts of LULC changes on meteorological forcings such as temperature, radiation fluxes, and near-surface wind speed. The forcing parameters required by WRF-Hydro are incoming shortwave radiation, incoming longwave radiation, specific humidity, 2 m air temperature, surface pressure, U-wind component, V-wind component, and precipitation. However, one of the limitations of this study is that we used the default Green Vegetation Factor (GVF) that may slightly impact heat and moisture fluxes. However, we assume that these slight uncertainties will not influence the results significantly since this study focuses on the impact of unprecedented episodes of extreme events.

Subsequently, we employed the WRF-Hydro model from May 2016 to May 2017 to assess its performance in reproducing the observed hydrological regime of Kerala. We assessed the model performance in reproducing mean and extreme discharge values. WRF-Hydro requires information at high resolution for the routing grid based on the aggregation factor (20 in our case). We used CartoDEM Version-3 R1 data downloaded from Bhuvan (ISRO) to generate high-resolution routing grid files and channels. We also generated Lake Parameter files to incorporate lakes in this region. Shuttle Radar Topography Mission waterbody data (obtained from https://earthexplorer.usgs.gov) were adopted to mask lakes and create a Lake Parameter file. All small and large reservoirs were treated as lakes, not parameterized reservoirs, except 9 major reservoirs (Kallada, Kakki, Periyar, Idukki, Idamalayar, Aliyar, Parambikulam, Malampuzha, and Sholayar) due to incomplete storage information for others. We obtained the storage data from INDIA-WRIS and incorporated the same in the Lake Parameterization file to activate level-pool routing and simulate the storage dynamics of the reservoirs. Using these high-resolution routing grid files and WRF-simulated forcing, except precipitation, we designed 4 experiments with WRF-Hydro, with LULC for 1985, 1995, 2005, and 2018. The WRF-Hydro simulations were initialized as warm-starts having 2 yr of spinup time. Since this study focuses on analyzing high-intensity rainfall, we used the 3-hourly satellite precipitation product 3B42V7 from Tropical Rainfall Measuring Mission (TRMM).

We identified 20 spatially distributed stations over Kerala using INDIA-WRIS hydro-met services. These stations record discharge data with daily frequency.

There are more than 40 large and small reservoirs in this region and over 44 rivers (INDIA-WRIS). The reservoirs regulate the flow by altering the natural river course. The simulation of regulated flow without enough prior information of reservoirs in the region is an intricate task. The operation of floodgates in this region plays a significant role in flooding. One of the caveats of our study is the lack of data availability of all reservoirs in the region. If there were limited/no role of reservoirs, the flooding impacts reported in this study would be different.

In this study, we were able to incorporate only 9 major reservoirs because of data unavailability for all others. Therefore, the model calibration, using all points, for such a large area with many non-parameterized reservoirs may lead to a false representation of hydrologic parameters. Thus, we selected 11 stations that are downstream and fall in the region critically affected by the 2018 flood. We validated WRF-Hydro performance at these stations with observed discharge from May 2016 to May 2017, the most recent observation data available (see Fig. S4 in the Supplement, www.int-res.com/articles/suppl/c089p001_supp.pdf). We examined hydrographs and flow duration curves of all 11 selected stations for each simulation. We analyzed spatial runoff, subsurface runoff, and evapotranspiration in this region for all LULC years and compared them to subsequent years. The flood inundation and surface water head were also analyzed to examine the impact of the event under changing LULC.

We highlight that WRF and WRF-Hydro were not run in coupled mode. WRF-Hydro was run in the isolation, whereby we used parameters mentioned above, having no feedback to WRF of any fluxes. We further highlight that the experiments are designed to reveal the extent that LULC changes influenced the impacts of this event. Therefore, if we force the WRF-simulated precipitation in WRF-Hydro, it may become an added source of uncertainty due to the differences in precipitation simulated under these experiments.

Table 2. Area (km^2) for dominant land use/land cover (LULC) classes in the Kerala region (India) that are important to hydrological responses

LULC class	1985	1995	2005	2018
Urban and Built-up Land	594	839	614	1282
Cropland and Pasture	2634	2636	4741	3223
Grassland	428	431	292	16
Shrubland	1441	1481	207	51
Evergreen Forest	5712	5511	3759	4084
Mixed Forest	22 075	22 164	21 216	14 622

4. RESULTS AND DISCUSSION

We first characterized the state of LULC and its conversion among different classes for 1985, 1995, 2005, and 2018. To assess the impact of LULC change on the flood event, we used discharge, surface runoff, sub-surface runoff, flood inundation, and surface head height from WRF-Hydro.

4.1. Observed changes in LULC

Table 2 lists the different classes in the LULC of 1985, 1995, 2005, and 2018. We observed an increasing trend in UBL throughout 1985–2018, with a small reduction from 1995 to 2005. Similar to this, BSV also showed an atypical low fractional area in 2005 (Fig. S1).

Considering 1985 as the baseline, the EF area decreased slightly in 1995 (~4 %) with a significant reduction in 2005 (32 %). EF exhibited a modest increment in 2018 (8 %), which could be because of various afforestation initiatives by the Kerala Government and NGOs. MF showed an almost negligible increasing trend in 1995 but experienced a reduction in 2005 (4 %) and 2018 (31 %). In the later part of the study period (2005–2018), EF and MF were converted to CLP, which led to an increment in CLP area. In 2018, CLP was reduced because Pasture and Mixed Grass Fields were converted to Barren Land. GL experienced a reduction in 2005 (32 %) and 2018 (94 %) with a small increment in 1995 (~1 %). SL also followed a similar trend and declined in 2005 (85 %) and 2018 (75 %) with little growth in 1995 (3 %). UBL showed significant growth in 1995 (41 %) and 2018 (108 %), with a reverse trend in 2005 (26 %). The urban built-up impervious area increased, while forest and native cover decreased substantially. An increase in impervious areas tends to reduce the travel time and increase the magnitude of the flood waves, thus producing severe impacts.

4.2. WRF-Hydro validation

Table 3 shows the skill measures comparing the observed and model-simulated discharge at the studied stations. A linear regression coefficient (R^2) ≥0.5 is broadly accepted and considered good (Santhi et al. 2001, Van Liew et al. 2003, Moriasi et al. 2007). We noted that 7 out of 11 stations show R^2 ≥0.4 and regard it as reasonable in this

Table 3. Accuracy measures of Weather Research Forecasting (WRF)/WRF-Hydro simulated discharge for various stations in Kerala (India) for May 2016 to May 2017. R^2: coefficient of determination; *D*: index of agreement; NSE: Nash-Sutcliffe efficiency coefficient; M_NSE: modified NSE; MDE: median error; MDAE: median absolute error; RMSE: root mean squared error

Station	R^2	*D*	NSE	M_NSE	MDE (cm)	MDAE (cm)	RMSE (cm)
Arangaly	0.3	0.7	0.3	0.3	6.2	10.1	34.7
Erinjipuzha	0.4	0.8	0.3	0.4	−3.9	6.8	66.1
Kalampur	0.3	0.6	0.2	0.3	0.7	14.4	33.8
Karathodu	0.6	0.7	0.5	0.6	0.1	0.2	24.8
Kumbidi	0.5	0.7	0.5	0.5	8.6	12.3	87.2
Kuniyili	0.4	0.8	0.3	0.4	−20.1	26.0	82.8
Kuttyadi	0.6	0.5	0.1	0.3	−3.1	3.2	31.9
Muthankera	0.4	0.7	0.4	0.4	−5.0	6.4	56.5
Neeleswaram	0.3	0.7	0.1	0.3	−5.4	29.3	128.4
Permannu	0.5	0.8	0.5	0.5	1.1	13.1	94.0
Pulanthole	0.4	0.6	0.3	0.4	−1.0	3.2	33.6

region, which lacks the incorporation of several reservoirs because of incomplete information. R^2 is also overly sensitive to the outliers caused by the additive and proportional difference between simulated and observed data (Legates & McCabe 1999, Santhi et al. 2001, Van Liew et al. 2003, Moriasi et al. 2007). We calculated median error, median absolute error, and root mean squared error to assess the simulated discharge model bias and error. We found that all of these error metrics are fairly acceptable (Table 3). The index of agreement between simulated and observed discharge, which can distinguish additive and proportional difference, mean, and variance of the observed and simulated values (Legates & McCabe 1999, Santhi et al. 2001, Van Liew et al. 2003, Moriasi et al. 2007), was within an acceptable range (Table 3) for the selected stations

4.3. WRF-Hydro simulated discharge

Table 4 presents the percentage change in accumulated discharge (simulated by WRF-Hydro) at different locations but with LULC conditions of 1985, 1995, 2005, and 2018, along with the meteorological conditions of the August 2018 event. The change in discharge corresponding to LULC change during 1985–1995, for the August 2018 event, at all the stations except Ayilam is nominal (within ±3%), consistent with minimal land cover changes. The discharge with LULC of 2005 (compared to 1995) shows a substantial increase (3~50%) for most of the stations, with Ayilam showing an increase of 400%, probably due to the encroachment into the forests (Fig. S1) that further migrated to pastures and cropland during 1995–2005. Erinjipuzha station (in the northernmost part of Kerala) shows almost no change for any of the 4 LULC classes considered, probably because of almost no changes in LULC in this part of the region. Kalloppara, Kumbidi, Mallakkara, Mankara, Pattazhy, Pudur, Pulanthole, and Thumpamon show increased discharge by more than 10%. In the LULC of 2018, compared to 2005, the increase in discharge at almost every station is modest (1~7%) except at Ayilam. This modest increase is consistent with small changes in LULC from 2005 to 2018, as noted earlier.

Fig. S2 shows the hydrographs of all the stations. The peak characteristic and variation for the various LULC scenarios are consistent with the information shown in Table 4. For most of the stations, the increase in discharge from 1995 to 2005 was higher than the changes in other decades (see Fig. S2). In 2005, the 10% exceedance flow (Q_{10}) increased by more than 10% for some stations (Kalloppara, Kumbidi, Mallakkara, Mankara, Pattazhy, Pulanthole, and Thumpamon). Q_{10} for Man-

Table 4. Percentage (%) change in August 2018 accumulated discharge (simulated by WRF-Hydro) at various stations across Kerala for land use/land cover conditions corresponding to 1985–1995, 1995–2005, and 2005–2018

Station	1985–1995	1995–2005	2005–2018	1995–2018
Arangaly	<1	8.8	−1.02	7.7
Ayilam	9.69	462.89	28.35	622
Erinjipuzha	<1	<1	<1	<1
Kalampur	<1	5.37	<1	5.32
Kalloppara	<1	11.22	<1	11.6
Karathodu	<1	5.79	<1	5.64
Kidangoor	<1	7.42	<1	7.14
Kumbidi	−1.21	14.21	2.16	16.67
Kuniyili	<1	3.43	<1	3.54
Kuttyadi	<1	5.71	<1	5.94
Mallakkara	<1	13.04	<1	13.56
Mankara	−2.24	37.76	7.31	47.83
Muthankera	<1	2.86	<1	2.97
Neeleswaram	<1	4.36	1.84	6.28
Pattazhy	2.41	52.31	1.16	54.1
Permannu	<1	2.87	<1	3.37
Pudur	<1	10.66	4.95	16.13
Pulanthole	−2.66	12.2	<1	12.1
Thumpamon	<1	38.79	<1	39.68
Vendiperiyar	<1	11	<1	11.48

kara shows an increase of almost 30%, while for Thumpanon and Pattazhy, the increase is approximately 40 and 56%, respectively (see Fig. S3).

4.4. Terrestrial water flux

Fig. 3 illustrates the accumulated surface runoff (in mm) for the August 2018 event, before channel routing, for LULC conditions of 1985, 1995, 2005, and 2018, and their differences. The surface runoff represents the amount of water available to be routed under different hydrologic components, e.g. overland flow routing, sub-surface routing, and channel routing. Fig. 4 represents accumulated subsurface runoff (in mm h^{-1}) during the August 2018 event for LULC of 1985, 1995, 2005, and 2018 and their differences. The subsurface runoff is inclusive of baseflow, vertical flow, and quasi flow between grid points. Fig. 5 depicts accumulated evapotranspiration (in mm h^{-1}) for August 2018 for LULC of 1985, 1995, 2005, and 2018, and their differences. The following subsections provide an explanation of these fluxes and their changes over the decades.

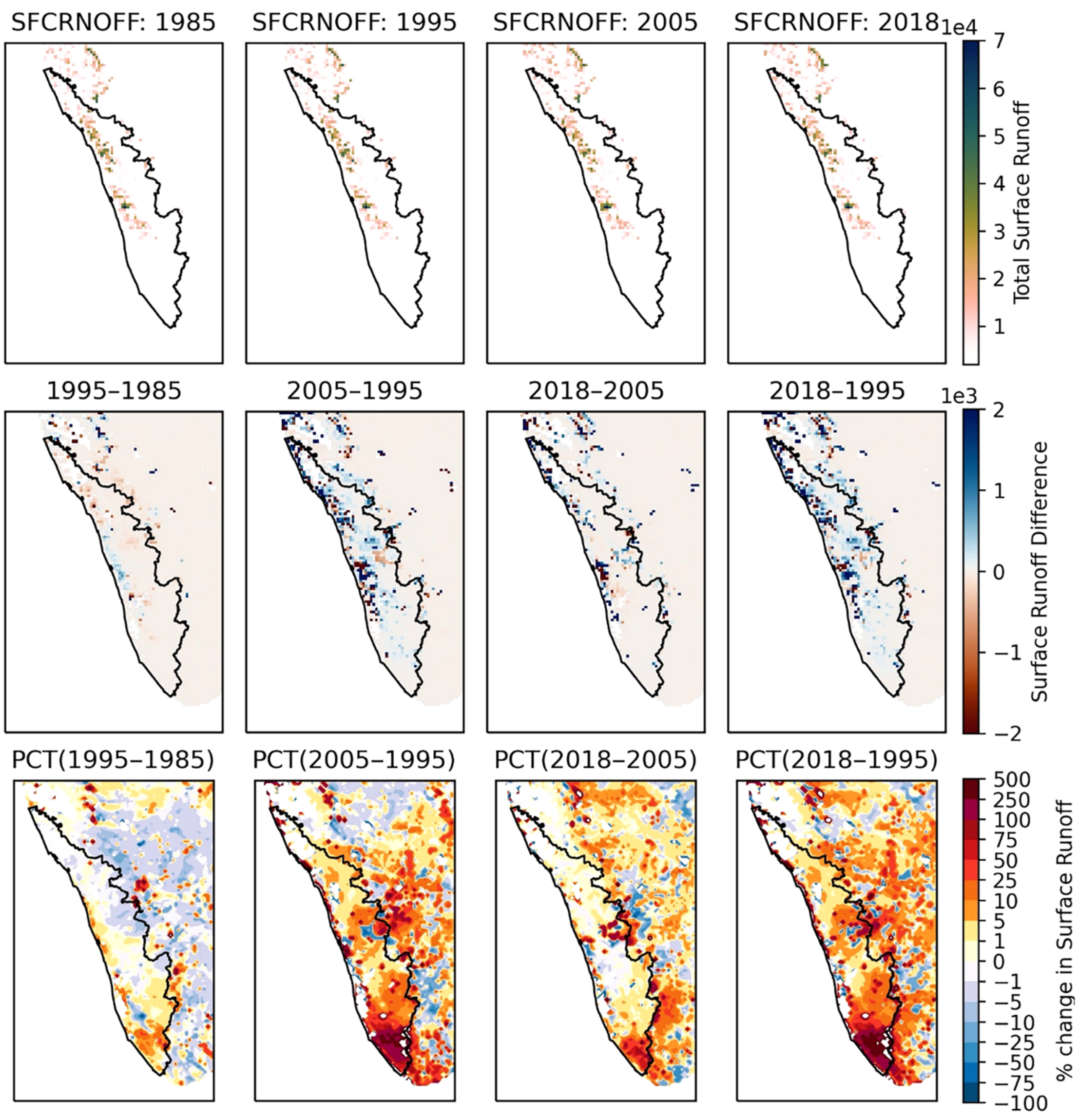

Fig. 3. Top row: total surface runoff (SFCRNOFF, in mm) for the August 2018 flooding event simulated by WRF-Hydro for land use/land cover (LULC) conditions of 1985, 1995, 2005, and 2018. Middle row: differences in the surface runoff (mm) for LULC changes corresponding to 1985–1995, 1995–2005, 2005–2018, and 1995–2018. Bottom row: differences in percentage (PCT) for the same 4 periods. The black line shows the state boundary of Kerala

4.4.1. 1985–1995

The difference in surface runoff between 1985 and 1995 LULC conditions (Fig. 3) is negligible across the entire state. However, we found subsurface runoff for 1995 LULC to be slightly higher (over part of the region that showed modest changes) than that of 1985 (Fig. 4), and evapotranspiration to have slightly decreased (as a consequence) for 1995 compared to 1985 (Fig. 5). These changes are likely due to urban expansion and a slight deforestation trend.

4.4.2. 1995–2005

Under the LULC of 2005, compared to 1995, the August 2018 event produced a significant increase in surface runoff (Fig. 3), subsurface runoff (Fig. 4), and a decrease in evapotranspiration (Fig. 5) over the entire state of Kerala. As noted, 1995~2005 saw the largest decline in vegetation cover, especially SL and GL, resulting in a reduction in vegetation cover compared to the previous period and increased bare soil exposure. These changes combine to increase infil-

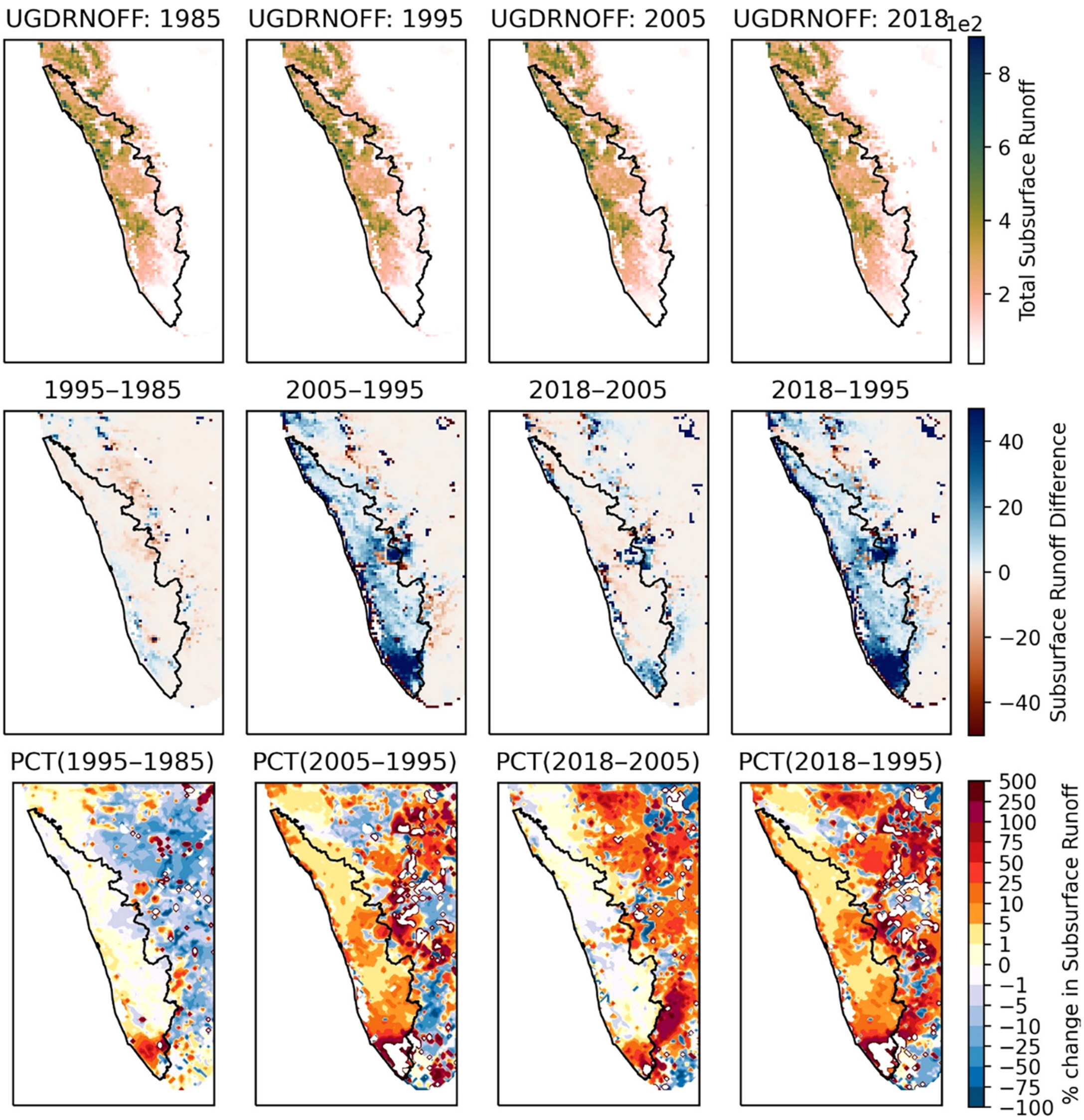

Fig. 4. As in Fig. 3, but for total sub-surface (underground) runoff (UGDRNOFF, in mm) for August 2018 event for land use/land cover (LULC) of 1985 (UGDRNOFF: 1985), 1995 (UGDRNOFF: 1995), 2005 (UGDRNOFF: 2005), and 2018 (UGDRNOFF: 2018). The difference in the sub-surface runoff (mm) for LULC changes corresponding to 1985–1995 is shown in (1995–1985), corresponding to 1995–2005 in (2005–1995), corresponding to 2005–2018 in (2018–2005), and corresponding to 1995–2018 in (2018–1995). The differences in percentage are shown in PCT(1995–1985), PCT(2005–1995), PCT(2018–2005), and PCT(2018–1995) for 1985–1995, 1995–2005, 2005–2018, and 1995–2018, respectively. The black boundary line bounds the Kerala region

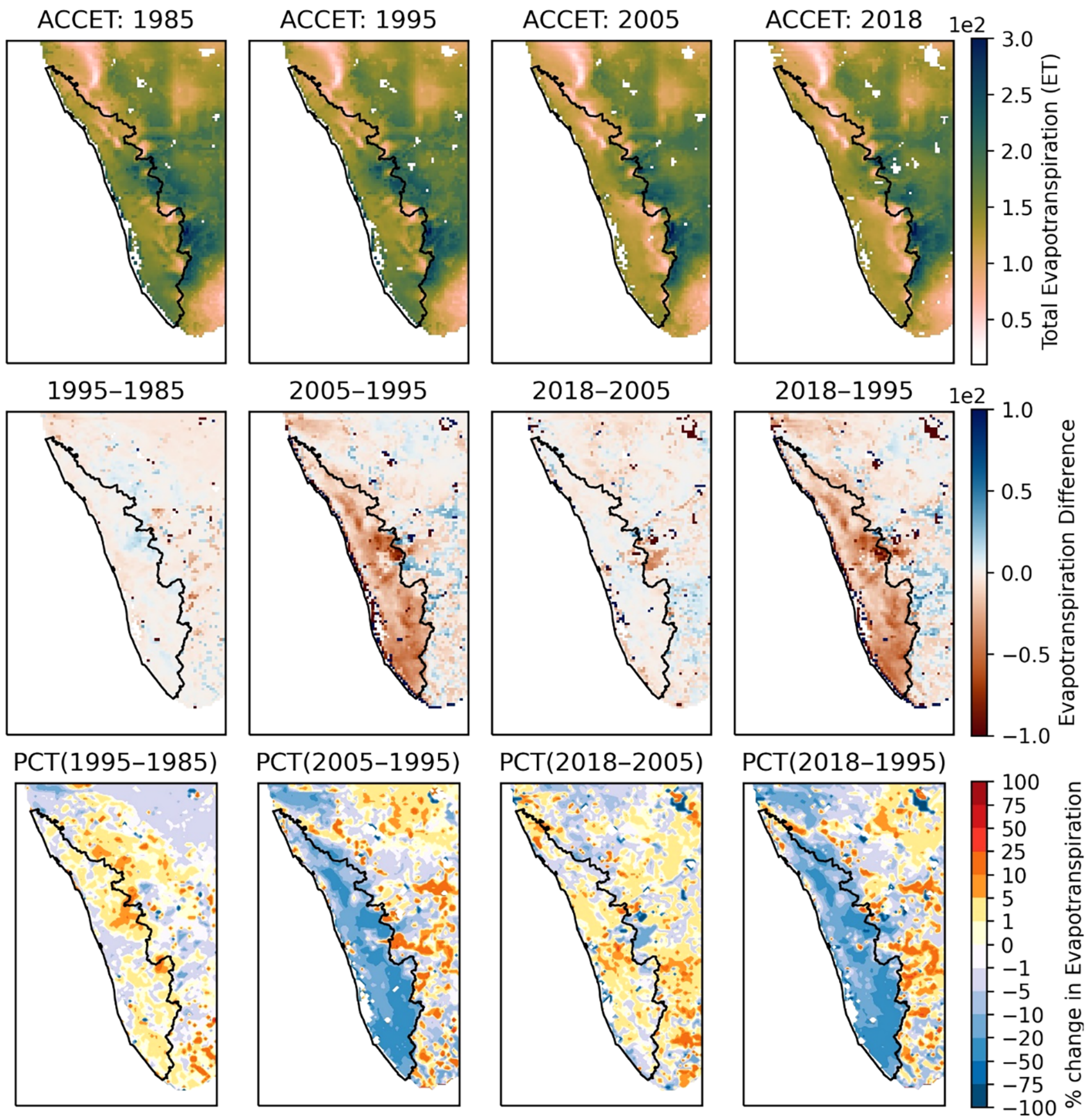

Fig. 5. As in Fig. 3, but for total accumulated evapotranspiration (ACCET, in mm)

tration and decrease evapotranspiration. Vegetation detains the water in the canopy, thereby reducing surface runoff and the peak in the runoff, but with decreasing vegetation, the surface runoff increases, as seen in Fig. 3.

4.4.3. 2005–2018

From 2005 to 2018, LULC changes were small, with a slowing of deforestation and even an increase in the total forest cover (India State of Forest Report 2019). Even these small results in surface runoff increase for the August 2018 event in some parts of Kerala compared to the LULC of 2005 (Fig. 3), especially areas of MF (Fig. 1), saw a modest reduction. Subsurface runoff for 2018 showed a mixed response, i.e. increasing in some parts and decreasing in others (Fig. 4), consistent with the LULC changes, with the magnitude of increase higher than the reduction. Evapotranspiration showed similar changes for 2018 (Fig. 5). Grid points with an increase in subsurface runoff show decreased evapotranspiration and vice versa, consistent with land cover changes.

We argue that changes in fluxes mostly respond to the continuing deforestation and destruction of SL and GL. An urban fraction has also expanded during this period that significantly alters these fluxes. The reverse trend (afforestation from 2005 to 2018) in EF is likely why some grid points show reduced subsurface runoff and increased evapotranspiration during the corresponding period.

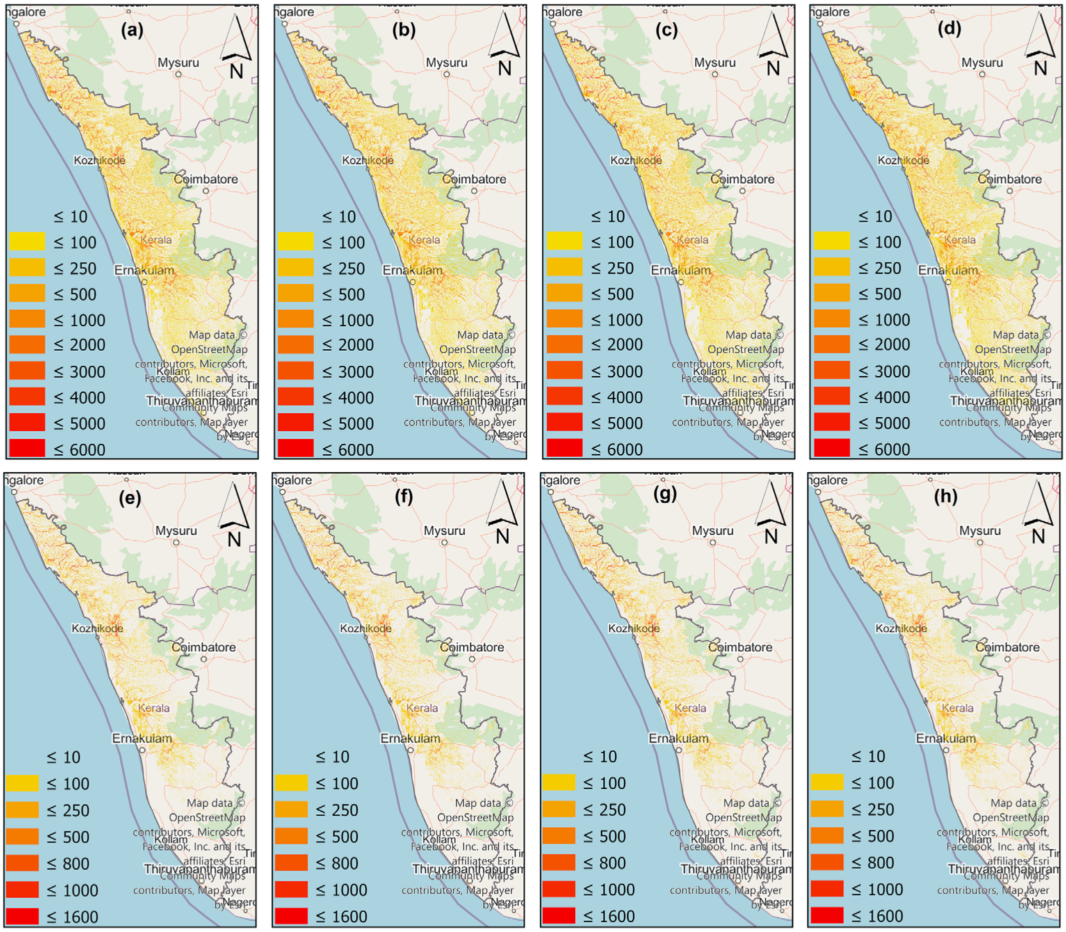

Fig. 6. Maximum surface water height (in mm) for the August 2018 flooding event simulated for land use/land cover (LULC) conditions of (a) 1985, (b) 1995, (c) 2005, and (d) 2018. Panels (e)–(h) show the corresponding maps for mean surface water height

4.5. Flood inundation

Fig. 6 illustrates the maximum and mean surface water height over Kerala for the August 2018 event under the different LULC scenarios. The maximum and mean water height is small with the 1985 or 1995 LULC (Fig. 6a,b,e,f); however, inundation is higher with the 2005 LULC, and minimal change is observed with the 2018 LULC (Fig. 6g,h). These results are consistent with the observed hydrologic flux changes.

To highlight the changes, we show the differences in water surface heights and duration of flooding between 1995–2018 and 2005–2018. We calculated flooding duration as the number of hours the water depth exceeds the water depth from the 2018 LULC . Relative to the 1995 LULC, the maximum water height and duration of flooding for the 2018 LULC is higher across the entire state of Kerala, although the changes in mean water height are small (Fig. 7a–c), consistent with high flood levels (Fig. 6). However, the changes in the flooding parameters are less for 2005–2018, consistent with the smaller changes in LULC over this period. There are parts with a negative mean for 2005–2018 changes that could correspond to the reversal in deforestation. Kerala showed a 25 % exceedance (computed for the 1995 LULC) for most of the time with the 2018 LULC. The corresponding increase for 2005 to 2018 is much smaller in extent as compared to 2018 versus 1995.

5. SUMMARY AND CONCLUSION

In this study, we have assessed the role of LULC changes from 1985 through 2018 on the mega-floods over Kerala, which occurred in August 2018. In the first step of this study, we performed an LULC change analysis over Kerala. We found a large reduction in green cover in this region, including EF, MF, SL, and GL. During the period 1995–2005, EF

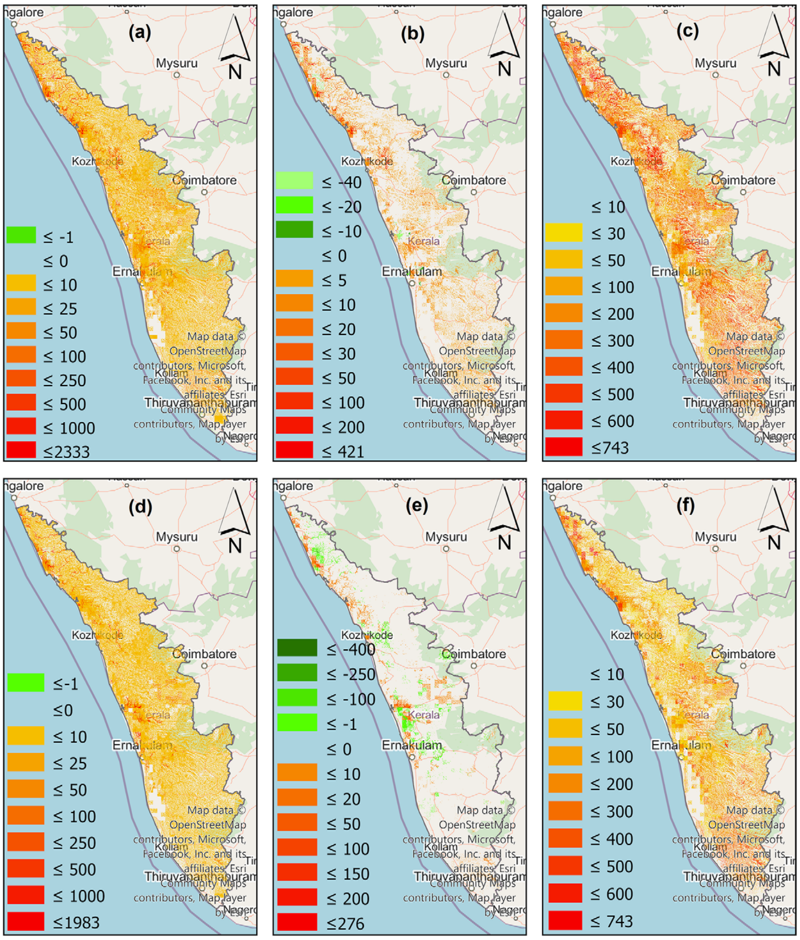

Fig. 7. Change in surface water height flux (in mm) for the August 2018 flooding event simulated for land use/land cover (LULC) changes corresponding to 1995–2018 for (a) maximum height, (b) mean height, and (c) total exceedance duration in hours. Panels (d)–(f) show the corresponding maps for LULC changes corresponding to 2005–2018

was heavily deforested, and parts of it transitioned to MF. MF showed maximum loss during the period 2005–2018.

We found increased surface and sub-surface runoff for the changes that occurred during 1985–2018; however, most of these changes occurred during the 11 yr period 1995–2005. The destruction in forest cover and green vegetation may have contributed to these hydrological changes in this region. Kerala observed increased runoff for few stations during 1985–1995 and 2005–2018, but for almost all stations during 1995–2005. In 2005, many stations witnessed higher Q_{10}. Many stations (Kalloppara, Kumbidi, Mallakkara, Mankara, Pattazhy, Pulanthole, and Thumpamon) were found to have an increment in Q_{10} of approximately 10%. One station (Mankara) showed an increase in Q_{10} of 30% and 2 stations of 40 and 56% (Thumpanon and Pattazhy, respectively).

A detailed analysis of flood inundation and surface water head for WRF-Hydro simulations in different parts of Kerala was carried out. We found that almost every part of Kerala experienced a higher duration of ponded water. While the increase was highest for LULC changes corresponding to 1995–2005, the increase was minimal for LULC changes corresponding to 1985–1995 and 2005–2018. A large part of Kerala experienced at least 25% of exceedance for a significant amount of time for 2018 LULC as compared to 1995 LULC, with many locations experiencing a large increase in duration even at 90% exceedance levels.

A broad conclusion drawn from this work is that the severity of the flood (measured in terms of inundation, discharge, and surface height) could have been lowered had Kerala not experienced massive destruction of forest cover and green cover. From 1995 to 2005, EF and MF showed a decreasing trend, with a higher rate of loss in EF compared to MF. Notably, the urban fraction showed a slight decline during the same period. During 2005–2018, EF showed a slightly increasing trend; however, there was a significant decreasing trend in the MF cover and increased urban fraction during the same period. Loss in SL and GL remained severe from 1995 to 2018. With the aforementioned green cover dynamics, we found the highest changes in hydrological fluxes during 1995–2005. The values of various flooding parameters indicate flooding with the 1985 LULC as well, but not as severe as for 2005 and 2018. Although the operation of floodgates of dams induced and escalated more flooding, the flood catastrophe was inevitable under any scenario of LULC change, climate change, or floodgate operations (Hunt & Menon 2020). These authors also reported a significant amplification in the intensity of the flood at the end of this century under the RCP8.5 projection scenario. While Hunt & Menon (2020) found amplification of flood intensity under atmospheric alterations, we found amplification under the influence of LULC changes. Since the primary objective this study was to investigate the role of LULC changes on the severity of the flooding event, we did not consider various operational scenarios for reservoirs. However, it would be interesting to investigate how different reservoir functional scenarios would have modified the impact on flooding due to LULC changes.

Acknowledgements. We thank the MoES, Govt. of India, for providing partial financial assistance as a fellowship under the IITD-MoES MoU on 'Capacity Building in the field of earth and atmospheric sciences' at CAS, IIT Delhi, and 'DST-FIST 2014' project grant at CAS. The DST Centre of Excellence in Climate Modeling at IIT Delhi (Project RP03350) is acknowledged for logistical support. We also thank the IIT Delhi HPC facility for computational resources. We acknowledge Bhuvan for the Digital Elevation Model (https://bhuvan.nrsc.gov.in). The waterbody boundary dataset was downloaded from https://earthexplorer.usgs.gov. Station discharge data and initial reservoir conditions were obtained from INDIA-WRIS (https://indiawris.gov.in/wris/). Decadal LULC was obtained from https://daac.ornl.gov/cgi-bin/dsviewer.pl?ds_id=1336, and initial and lateral boundary conditions for WRF from https://rda.ucar.edu/.

LITERATURE CITED

Rajiv Gandhi Institute of Development Studies (2018) Kerala Flood 2018: the disaster of the century Rajiv Gandhi Institute of Development Studies. https://sdma.kerala.gov.in/wp-content/uploads/2020/08/Rajeev-Gandhi-Centre-Kerala-flood-2018-The-disaster-of-the-century.pdf (accessed 26 May 2022)

Alexander LV, Zhang X, Peterson TC, Caesar J and others (2006) Global observed changes in daily climate extremes of temperature and precipitation. J Geophys Res 111:D05109

Allan RP, Soden BJ (2008) Atmospheric warming and the amplification of precipitation extremes. Science 321: 1481–1484

Bhaduri B, Harbor J, Engel B, Grove M (2000) Assessing watershed-scale, long-term hydrologic impacts of land-use change using a GIS-NPS model. Environ Manag 26: 643–658

Biswadip G (2014) IRS-P6 AWiFS derived gridded land use/land cover data compatible to mesoscale models (MM5 and WRF) over Indian region. NRSC Tech Doc NRSC-ECSA-ACSG-OCT-2014-TR-651. National Remote Sensing Centre, Hyderabad

Boyaj A, Dasari HP, Hoteit I, Ashok K (2020) Increasing heavy rainfall events in south India due to changing land use and land cover. Q J R Meteorol Soc 146:3064–3085

Bubeck P, Otto A, Weichselgartner J (2017) Societal impacts of flood hazards. Oxford Research Encyclopedia of Natural Hazard Science 1, doi:10.1093/acrefore/9780199389407.013.281

Chahine MT (1992) The hydrological cycle and its influence on climate. Nature 359:373–380

Cheng Y, Parlange MB, Brutsaert W (2005) Pathology of Monin-Obukhov similarity in the stable boundary layer. J Geophys Res Atmos 110:D06101

Chevuturi A, Dimri AP (2016) Investigation of Uttarakhand (India) disaster-2013 using weather research and forecasting model. Nat Hazards 82:1703–1726

Das P, Behera MD, Patidar N, Sahoo B and others (2018) Impact of LULC change on the runoff, base flow and evapotranspiration dynamics in eastern Indian river basins during 1985–2005 using variable infiltration capacity approach. J Earth Syst Sci 127:19

Deb SK, Srivastava TP, Kishtawal CM (2008) The WRF model performance for the simulation of heavy precipitating events over Ahmedabad during August 2006. J Earth Syst Sci 117:589–602

Diffenbaugh NS, Singh D, Mankin JS, Horton DE and others (2017) Quantifying the influence of global warming on unprecedented extreme climate events. Proc Natl Acad Sci USA 114:4881–4886

Dudhia J (1989) Numerical study of convection observed during the Winter Monsoon Experiment using a mesoscale two-dimensional model. J Atmos Sci 46:3077–3107

Frans C, Istanbulluoglu E, Mishra V, Munoz-Arriola F, Lettenmaier DP (2013) Are climatic or land cover changes the dominant cause of runoff trends in the Upper Mississippi River Basin? Geophys Res Lett 40:1104–1110

Frumkin H (2002) Urban sprawl and public health. Public Health Rep 117:201–217

Gadgil M, Krishnan BJ, Geneshaiah KN, Vijayan VS and others (2011) Report of the Western Ghats Ecology Expert Panel, Part I. https://ruralindiaonline.org/en/library/resource/report-of-the-western-ghats-ecology-expert-panel/

Gochis DJ, Barlage M, Dugger A, FitzGerald K and others (2018) The NCAR WRF-Hydro modeling system technical description (Version 5.0). NCAR Tech Note. https://ral.ucar.edu/sites/default/files/public/WRF-HydroV5TechnicalDescription.pdf

Goswami BN, Venugopal V, Sengupta D, Madhusoodanan MS, Xavier PK (2006) Increasing trend of extreme rain events over India in a warming environment. Science 314:1442–1445

Government of Kerala (2018) Kerala Floods — 2018, 1st August to 30th August 2018. State Relief Commissioner, Disaster Management, Government of Kerala. https://sdma.kerala.gov.in/wp-content/uploads/2019/08/Memorandum2-Floods-2018.pdf (accessed 15 July 2021)

Hong SY, Lim J (2006) The WRF single-moment 6-class microphysics scheme (WSM6). Asia Pac J Atmos Sci 42:129–151

Hong SY, Noh Y, Dudhia J (2006) A new vertical diffusion package with an explicit treatment of entrainment processes. Mon Weather Rev 134:2318–2341

Hunt KMR, Menon A (2020) The 2018 Kerala floods: a climate change perspective. Clim Dyn 54:2433–2446

India State of Forest Report (2019) Forest Survey of India. Ministry of Environment, Forest & Climate Change Government of India, Dehradun

IPCC (Intergovernmental Panel on Climate Change) (2007) Climate Change 2007: synthesis report. Contribution of Working Groups I, II and III to the Fourth Assessment Report of the Intergovernmental Panel on Climate Change. IPCC, Geneva

Jayakumar PB (2018) Flood-ravaged businesses in Kerala stare at Rs 40,000 crore losses. Business Today. https://www.businesstoday.in/current/economy-politics/kerala-flood-businesses-stare-at-rs-40000-crore-loss/story/281765.html

JRDNA Team (Joint Rapid Damage and Needs Assessment Team) (2018) Kerala floods and landslides 2018. Joint Rapid Damage and Needs Assessment Report Septem-

ber 2018. https://sdma.kerala.gov.in/wp-content/uploads/2020/08/Master_Kerala_JRDNA_Oct-12-1.pdf (accessed 15 July 2021)
Kain JS (2004) The Kain–Fritsch convective parameterization: an update. J Appl Meteorol 43:170–181
Kumar A, Dudhia J, Rotunno R, Niyogi D, Mohanty UC (2008) Analysis of the 26 July 2005 heavy rain event over Mumbai, India using the Weather Research and Forecasting (WRF) model. Q J R Meteorol Soc 134:1897–1910
Legates DR, McCabe GJ Jr (1999) Evaluating the use of 'goodness-of-fit' measures in hydrologic and hydroclimatic model validation. Water Resour Res 35:233–241
Lehmann J, Coumou D, Frieler K (2015) Increased record-breaking precipitation events under global warming. Clim Change 132:501–515
Li Y, Wang C (2009) Impacts of urbanization on surface runoff of the Dardenne Creek watershed, St. Charles County, Missouri. Phys Geogr 30:556–573
Mahmood R, Pielke RA Sr, Hubbard KG, Niyogi D and others (2010) Impacts of land use/land cover change on climate and future research priorities. Bull Am Meteorol Soc 91:37–46
Mayaja NA, Srinivasa CV (2016) Land use and land cover changes and their impacts on floods in Pampa River Basin in Kerala: a remote sensing based analysis. In: Raju NJ (ed) Geostatistical and geospatial approaches for the characterization of natural resources in the environment. Springer International Publishing, Cham, p 779–783
Millennium Ecosystem Assessment (2005) Ecosystems and human well-being: synthesis. Island Press, Washington, DC
Mishra V, Shah HL (2018) Hydroclimatological perspective of the Kerala Flood of 2018. J Geol Soc India 92:645–650
Mishra V, Cherkauer KA, Niyogi D, Lei M, Pijanowski BC, Ray DK, Bowling LC and others (2010) A regional scale assessment of land use/land cover and climatic changes on water and energy cycle in the upper Midwest United States. Int J Climatol 30:2025–2044
Mlawer EJ, Taubman SJ, Brown PD, Iacono MJ, Clough SA (1997) Radiative transfer for inhomogeneous atmospheres: RRTM, a validated correlated-k model for the longwave. J Geophys Res Atmos 102:16663–16682
Moriasi DN, Arnold JG, Van Liew MW, Bingner RL, Harmel RD, Veith TL (2007) Model evaluation guidelines for systematic quantification of accuracy in watershed simulations. Trans ASABE (Am Soc Agric Biol Eng) 50:885–900
Nie W, Yuan Y, Kepner W, Nash MS, Jackson M, Erickson C (2011) Assessing impacts of landuse and landcover changes on hydrology for the upper San Pedro watershed. J Hydrol 407:105–114
Niu GY, Yang ZL, Mitchell KE, Chen F and others (2011) The community Noah land surface model with multiparameterization options (Noah-MP).: 1. Model description and evaluation with local-scale measurements. J Geophys Res Atmos 116:D12109
Novotny V, Olem H (1994) Water quality: prevention, identification, and management of diffuse pollution. Van Nostrand Reinhold, 1994), New York, NY
Petchprayoon P, Blanken PD, Ekkawatpanit C, Hussein K (2010) Hydrological impacts of land use/land cover change in a large river basin in central-northern Thailand. Int J Climatol 30:1917–1930
Piao S, Friedlingstein P, Ciais P, de Noblet-Ducoudré N, Labat D, Zaehle S (2007) Changes in climate and land use have a larger direct impact than rising CO2 on global river runoff trends. Proc Natl Acad Sci 104:15242–15247
Prasad G, Ramesh MV (2019) Spatio-temporal analysis of land use/land cover changes in an ecologically fragile area — Alappuzha District, Southern Kerala, India. Nat Resour Res 28:31–42
Rajiv Gandhi Institute of Development Studies (2018) Kerala Flood 2018: the disaster of the century. https://sdma.kerala.gov.in/wp-content/uploads/2020/08/Rajeev-Gandhi-Centre-Kerala-flood-2018-The-disaster-of-the-century.pdf (accessed on 26 May 2022)
Roxy MK, Ghosh S, Pathak A, Athulya R and others (2017) A threefold rise in widespread extreme rain events over central India. Nat Commun 8:708
Roy PS, Meiyappan P, Joshi PK, Kale MP and others (2016) Decadal land use and land cover classifications across India, 1985, 1995, 2005. ORNL DAAC, Oak Ridge, TN. https://doi.org/10.3334/ORNLDAAC/1336
Santhi C, Arnold JG, Williams JR, Dugas WA, Srinivasan R, Hauck LM (2001) Validation of the SWAT model on a large river basin with point and nonpoint sources. J Am Water Resour Assoc 37:1169–1188
Shaji J, Sajith SL, Joseph J, Ramachandran KK (2017) LULC change along Central Kerala coast and perception on implementation of CRZ notification. National Conference on Geospatial Technology, 12th & 13th January 2017, LBS Institute of Technology for Women, Thiruvananthapuram
Stott PA, Christidis N, Otto FEL, Sun Y and others (2016) Attribution of extreme weather and climate-related events. Wiley Interdiscip Rev Clim Change 7:23–41
Thomas J, Prasannakumar V (2016) Temporal analysis of rainfall (1871–2012) and drought characteristics over a tropical monsoon-dominated State (Kerala) of India. J Hydrol 534:266–280
UNDP (United Nations Development Programme) (2018) Post-disaster needs assessment – Kerala. https://www.undp.org/publications/post-disaster-needs-assessment-kerala (accessed 15 July 2021)
Wang W, Barker D, Bruyère C, Duda M and others (2008) WRF Version 3 Modeling System User's Guide. https://www2.mmm.ucar.edu/wrf/users/
Weng Q (2001) Modeling urban growth effects on surface runoff with the integration of remote sensing and GIS. Environ Manag 28:737–748
Wu F, Zhan J, Su H, Yan H, Ma E (2015) Scenario-based impact assessment of land use/cover and climate changes on watershed hydrology in Heihe River Basin of Northwest China. Adv Meteorol 2015:410198
Zhu C, Li Y (2014) Long-term hydrological impacts of land use/land cover change from 1984 to 2010 in the Little River Watershed, Tennessee. Int Soil Water Conserv Res 2:11–21
Zope PE, Eldho TI, Jothiprakash V (2016) Impacts of land use–land cover change and urbanization on flooding: a case study of Oshiwara River Basin in Mumbai, India. CATENA 145:142–154

Editorial responsibility: Oliver Frauenfeld, College Station, Texas, USA
Reviewed by: 3 anonymous referees

Submitted: January 11, 2021
Accepted: July 1, 2022
Proofs received from author(s): October 1, 2022